J|A|C|S COMMUNICATIONS

Published on Web 06/07/2010

# Controlling the Shapes of Silver Nanocrystals with Different Capping Agents

Jie Zeng,[†] Yiqun Zheng,[†] Matthew Rycenga,[†] Jing Tao,[‡] Zhi-Yuan Li,[§] Qiang Zhang,[†] Yimei Zhu,[‡] and Younan Xia*,[†]

*Department of Biomedical Engineering, Washington University, St. Louis, Missouri 63130, Condensed Matter Physics and Materials Science Department, Brookhaven National Laboratory, Upton, New York 11973, and Institute of Physics, Chinese Academy of Sciences, Beijing 100080, P. R. China*

Received April 29, 2010; E-mail: xia@biomed.wustl.edu

Shape control has proven to be a powerful and versatile means for tailoring the properties of metal nanocrystals for a wide variety of applications ranging from plasmonics[1] to sensing,[2] surface-enhanced Raman scattering (SERS),[3] imaging,[4] and catalysis.[5] Thanks to the efforts from many research groups, great progress has been made on this subject over the past decade. With Ag as a model system, we have demonstrated that the shape of a metal nanocrystal is determined primarily by the number of twin defects included in the seed.[6] However, for single-crystal seeds, they can still evolve into nanocrystals with different shapes such as cubes, truncated cubes, and octahedrons. In these cases, the capping agent plays a critical role in controlling the ratio of growth rates for {111} and {100} crystallographic planes and thus determining the final shape displayed by the product. For example, it has been shown that both poly(vinyl pyrrolidone) (PVP) and $Br^-$ ions can selectively bind to {100} facets of Ag to slow down their growth rate, resulting in the formation of nanocubes and nanobars.[7] On the contrary, citrate has been shown to bind more strongly to {111} than {100} facets, favoring the formation of nanoplates with a large portion of {111} facets on the surface.[8] Although these studies have contributed to our understanding of the role played by a capping agent in shape control, it should be pointed out that all of these experiments were conducted under different conditions so it is impossible to rule out the possible influence of other parameters.

In addressing this issue, we have designed a set of experiments based on seeded growth to single out the role of a capping agent (see Figure S1 in the Supporting Information for a schematic). The experiments were performed under identical conditions (e.g., seed, precursor, temperature, reductant, and concentrations of the reagents) except for the use of different capping agents. We found that two distinct shapes, namely, nanoscale octahedrons enclosed by {111} facets and nanocubes/nanobars covered by {100} facets, could be selectively and routinely produced by adding citrate and PVP, respectively, as the capping agent. This work provides a versatile approach to controlling the shape of metal nanocrystals by varying the capping agent while other parameters are kept the same.

Figure 1A and B show TEM and high-resolution TEM (HRTEM) images of single-crystal Ag nanocrystals with a spherical shape and an average diameter of 28 nm that were used as the seeds.[9] When sufficient $AgNO_3$ was introduced and reduced by L-ascorbic acid (AA) in the presence of sodium citrate ($Na_3CA$) in an aqueous solution at room temperature, we obtained Ag octahedrons of ~40 nm in edge length. Figure 1C and D show typical TEM and HRTEM images of the product. The fringe spacing of 1.4, 2.0, and 2.4 Å can be indexed to the {220}, {200}, and {111} reflections, respectively, of face-centered cubic (*fcc*) Ag. The selected area electron diffraction (SAED) pattern from the same nanoparticle (Figure 1D, inset) indicates that it was a piece of a single crystal sitting against a plane perpendicular to the [110] zone axis, confirming an octahedral shape with {111} facets exposed on the surface. Interestingly, by substituting $Na_3CA$ with PVP, the same Ag seeds ultimately grew into a mixture of nanocubes (25%) and slightly elongated nanocubes or nanobars (75%) with {100} facets exposed on the surface (Figure 1E and F). The SAED pattern in the inset of Figure 1F shows a square symmetry and spots for both {200} and {220} reflections, indicating that the particle was sitting on the TEM grid against one of its {100} facets. The three-dimensional shape of an elongated nanocube was also confirmed by TEM images taken at different tilting angles (Figure S2).

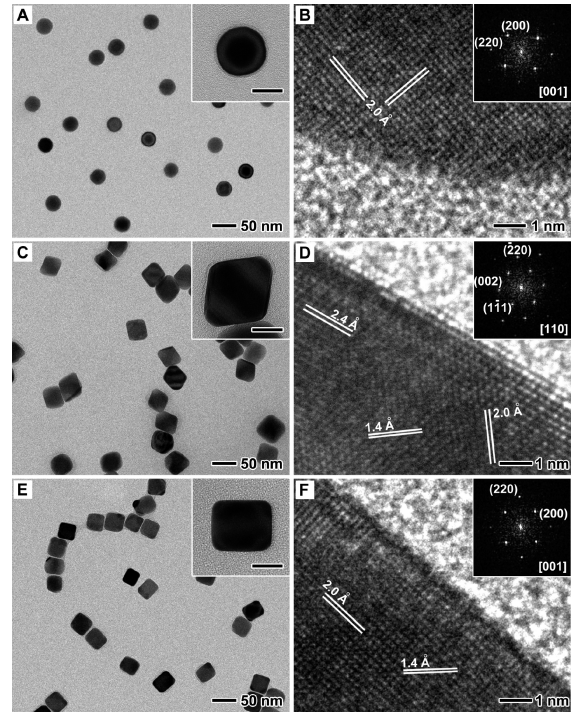


***Figure 1.*** (A) TEM and (B) HRTEM images of the spherical, single-crystal Ag seeds. (C) TEM and (D) HRTEM images of Ag octahedrons obtained by adding 1.8 mL of $AgNO_3$ into 2.1 mL of the Ag seeds, together with 0.1 mL of 40 mM AA and 0.8 mL of 40 mM $Na_3CA$. (E) TEM and (F) HRTEM images of Ag nanocubes and nanobars prepared under the same conditions as those for (C) except that 0.8 mL of 112 mM PVP (in terms of the repeating unit) was added instead of $Na_3CA$. The scale bars in the insets correspond to 20 nm.

Our previous studies (both theoretical and experimental) suggest that citrate could bind more strongly to {111} facets than {100} facets of *fcc* Ag at room temperature.[10] This difference in binding

[†] Washington University.
[‡] Brookhaven National Laboratory.
[§] Chinese Academy of Sciences.



10.1021/ja103655f 

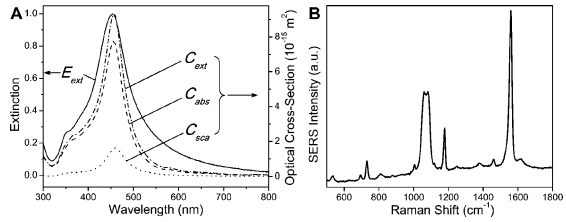


***Figure 2.*** (A) Normalized UV−vis spectrum ($E_{ext}$) of an aqueous suspension of the nanoscale Ag octahedrons, together with the extinction ($C_{ext}$), absorption ($C_{abs}$), and scattering ($C_{sca}$) spectra calculated using DDA method for a 40-nm Ag octahedron suspended in water with random orientations. For the DDA calculation, the corners of the octahedron were snipped by a sphere with a radius of 23 nm to better fit the real sample. (B) Solution-phase SERS spectrum of 1,4-BDT adsorbed on the surface of the Ag octahedrons.

energy is stipulated by two factors: (*i*) coincidence of the symmetries of the ligand and the Ag(111) surface and (*ii*) matching in dimensions for the ligand and the surface lattice constant. Accordingly, the {111} facets are expected to grow more slowly than the {100} facets during a seeded growth process when $Na_3CA$ is present. As such, the {100} facets will disappear gradually while the {111} facets will become more dominant, eventually leading to the formation of Ag octahedrons. As clearly shown in Figure S3, a mixture of cuboctahedrons and truncated octahedrons were obtained when we added a smaller amount (1.0 mL vs 1.8 mL) of $AgNO_3$ while other parameters were kept the same as in Figure 1C. Both of these nanocrystals had an increased ratio of {111} to {100} facets on the surface than the starting seeds, but the supply of Ag atoms was not sufficient for the seeds to evolve into octahedrons. Unlike citrate, PVP binds more strongly to {100} than {111} facets of *fcc* Ag[7a] and can thereby reduce the growth rate along the [100] direction. It makes the {111} facets disappear more quickly than the {100} facets, resulting in nanocubes and nanobars. According to our previous study, Ag nanobars could only be obtained by using $Br^-$ to promote the anisotropic growth, possibly via oxidative etching at a high temperature.[7b] In the present work, however, no $Br^-$ was introduced and the synthesis was conducted at room temperature. Interestingly, when 30-nm Ag nanocubes were used as the seeds for additional growth in the presence of $Na_3CA$, nanoscale Ag octahedrons were also obtained (Figure S4). This observation provides additional evidence to support our proposed mechanism; that is, the shape of a metal nanocrystal will be dictated by the capping agent as long as the seeds are single crystalline.

It should be pointed out that the Ag octahedrons that have been reported in literature all had edge lengths > 250 nm, because no capping agent like $Na_3CA$ for {111} facets was involved.[11] The availability of Ag octahedrons with truly nanoscale dimensions allows us to investigate their optical properties, for the first time. Figure 2A shows a normalized UV−vis spectrum ($E_{ext}$) recorded from an aqueous suspension of the as-synthesized nanoscale Ag octahedrons, which gave a strong localized surface plasmon resonance (LSPR) peak at ∼455 nm. There was also a shoulder peak at ∼365 nm. A comparison with the spectra calculated using the discrete-dipole approximation (DDA) method[12] indicates that the main peak is one of the dipole modes concentrating at the corners while the shoulder peak is another one distributing on the edges. The calculated and experimentally measured spectra match well in terms of peak positions and relative intensities. Note that the absorption ($C_{abs}$) contributes predominantly to the extinction ($C_{ext}$) for Ag octahedrons of such a small size. For the mixture of Ag nanocubes and nanobars, the UV−vis spectrum exhibits two major peaks (Figure S5A), corresponding to the nanocubes and the transverse mode at ∼430 nm and the longitudinal mode at ∼570 nm, respectively.

The well-defined nanocrystals were further investigated for SERS applications, as shown in Figure 2B for the octahedrons and in Figure S5B for the nanobars. We performed the measurements with 1,4-benzenedithiol (1,4-BDT) as the probe molecule and a 514 nm laser for excitation. Based on the 9a ring breathing mode (at 1182 $cm^{-1}$),[13] the enhancement factors (EFs) were calculated as $1.1 \times 10^4$ for the nanoscale octahedrons and $8.6 \times 10^4$ for the nanobars. Compared to the previous study, the EF of octahedrons is 1 order of magnitude higher than that of the anisotropically truncated octahedrons (with roughly the same dimensions) reported previously.[14] This difference arose because each of the corners is opposite to a flat face for the anisotropically truncated octahedron, while all of them are located at opposite positions for an octahedron, thus leading to a stronger dipole polarization.

In summary, we have demonstrated the use of seeded growth for directly comparing, for the first time, the effects of capping agents on shape control for Ag nanocrystals. We found that octahedral and cubic shapes could be selectively obtained by introducing $Na_3CA$ and PVP, respectively, as the capping agent. We expect this method could be further extended to quickly screen and evaluate the facet selectivity of a capping agent.

**Acknowledgment.** This work was supported by the NSF (DMR-0804088). Part of the work was performed at the Nano Research Facility, a member of the National Nanotechnology Infrastructure Network (NNIN), which is supported by the NSF under Award ECS-0335765. Work at BNL was supported by the U.S. DOE/BES under Contract No. DE-AC02-98CH10886.

**Supporting Information Available:** Experimental procedures, TEM and HRTEM images of other samples, tilted TEM images of a Ag nanobar, UV−vis and SERS spectra taken from Ag nanobars. This material is available free of charge via the Internet at http://pubs.acs.org.

## References

(1) (a) El-Sayed, M. A. *Acc. Chem. Res.* **2001**, *34*, 257. (b) Hutter, E.; Fendler, J. H. *Adv. Mater.* **2004**, *16*, 1685.
(2) (a) Haes, A. J.; Haynes, C. L.; McFarland, A. D.; Schatz, G. C.; Van Duyne, R. P.; Zou, S. *MRS Bull.* **2005**, *30*, 368. (b) Willets, K. A.; Van Duyne, R. P. *Annu. Rev. Phys. Chem.* **2007**, *58*, 267.
(3) (a) Cao, Y. C.; Jin, R.; Mirkin, C. A. *Science* **2002**, *297*, 1536. (b) Haynes, C. L.; McFarland, A. D.; Van Duyne, R. P. *Anal. Chem.* **2005**, *77*, 338A.
(4) (a) Chen, J.; Saeki, F.; Wiley, B. J.; Cang, H.; Cobb, M. J.; Li, Z.-Y.; Au, L.; Zhang, H.; Kimmey, M. B.; Li, X.; Xia, Y. *Nano Lett.* **2005**, *5*, 473. (b) Loo, C.; Lowery, A.; Halas, N.; West, J.; Drezek, R. *Nano Lett.* **2005**, *5*, 709.
(5) (a) Narayanan, R.; El-Sayed, M. A. *Nano Lett.* **2004**, *4*, 1343. (b) Wang, C.; Daimon, H.; Onodera, T.; Koda, T.; Sun, S. *Angew. Chem., Int. Ed.* **2008**, *47*, 3588. (c) Peng, Z.; Yang, H. *Nano Today* **2009**, *4*, 143. (d) Zhang, J.; Yang, H.; Fang, J.; Zou, S. *Nano Lett.* **2010**, *10*, 638. (e) El-Sayed, I. H.; Huang, X.; El-Sayed, M. A. *Nano Lett.* **2005**, *5*, 829.
(6) Wiley, B.; Sun, Y.; Xia, Y. *Acc. Chem. Res.* **2007**, *40*, 1067.
(7) (a) Sun, Y.; Mayers, B.; Herricks, T.; Xia, Y. *Nano Lett.* **2003**, *3*, 955. (b) Wiley, B. J.; Chen, Y.; McLellan, J. M.; Xiong, Y.; Li, Z.-Y.; Ginger, D.; Xia, Y. *Nano Lett.* **2007**, *7*, 1032.
(8) (a) Jin, R. C.; Cao, Y. W.; Mirkin, C. A.; Kelly, K. L.; Schatz, G. C.; Zheng, J. G. *Science* **2001**, *294*, 1901. (b) Jin, R. C.; Cao, Y. C.; Hao, E.; Metraux, G. S.; Schatz, G. C.; Mirkin, C. A. *Nature* **2003**, *425*, 487.
(9) Zhang, Q.; Li, W.; Wen, L.; Chen, J.; Xia, Y. *Chem.—Eur. J.* **2010**, DOI: 10.1002/chem.201000341.
(10) (a) Kilin, D. S.; Prezhdo, O. V.; Xia, Y. *Chem. Phys. Lett.* **2008**, *458*, 113. (b) Sun, Y.; Mayers, B.; Xia, Y. *Nano Lett.* **2003**, *3*, 675.
(11) Tao, A.; Sinsermsuksakul, P.; Yang, P. D. *Angew. Chem., Int. Ed.* **2006**, *45*, 4597.
(12) Zhou, F.; Li, Z. Y.; Liu, Y.; Xia, Y. *J. Phys. Chem. C.* **2008**, *112*, 20233.
(13) Rycenga, M.; Kim, M. H.; Camargo, P. H. C.; Cobley, C.; Li, Z. Y.; Xia, Y. *J. Phys. Chem. A* **2009**, *113*, 3932.
(14) Cobley, C.; Rycenga, M.; Zhou, F.; Li, Z.-Y.; Xia, Y. *Angew. Chem., Int. Ed.* **2009**, *48*, 4824.

JA103655F